以數位信號處理器為核心的磁浮系統之二維模糊滑動模式控制

Two-Dimensional Fuzzy Sliding Mode Control of DSP-Based Magnetic Levitation System

李振興 [1]
Jen-Hsing Li
崑山科技大學 電機系
ljh0906@mail.ksu.edu.tw

吳明芳 [2]
Ming-Fang Wu
崑山科技大學 電機系

摘 要

磁浮系統有很多工程上的應用，包括磁浮軸承、磁浮風洞、磁浮列車與半導體的磁浮抗震平台。磁浮系統是非線性系統，而且是開回路不穩定系統，必須有適當的控制才能維持穩定平衡，因此磁浮系統也可以測試控制理論的適用性。本文提出以數位信號處理器爲核心的磁浮系統之二維模糊滑動模式控制，模糊規則考慮滑動面與滑動面的導數。模糊滑動模式控制即是結合模糊邏輯控制與滑動模式控制所產生的控制方法。模糊滑動模式控制將模糊邏輯方法結合到滑動模式控制，因此保有滑動模式控制的優點也將模糊規則化簡到最少。由實驗的結果可知本方法有效的改善磁浮系統的性能響應。本文可以作爲控制系統教學的參考教材。

關鍵字：磁浮系統、模糊滑動模式控制、數位信號處理器、二維、控制系統教學。

Abstract

Magnetic levitation systems have widely used in many engineering applications, i.e. levitation of high speed trains, frictionless bearings, wind tunnels, and vibration isolation tables in semiconductor manufacturing. Magnetic levitation systems are nonlinear and open loop unstable systems. Hence, they are excellent educational tools for testing different control theories.

This paper proposes the two-dimensional fuzzy sliding mode control of DSP-based magnetic levitation system. The sliding manifold and its derivative are both considered for fuzzy rules. The fuzzy sliding mode control integrates the sliding mode control and fuzzy logic control. It has advantages of the sliding mode control and it can minimize rules of the fuzzy control. For the experimental results, this method improves responses of the magnetic levitation system effectively.

Keywords: magnetic levitation system, fuzzy sliding mode control, digital signal processor, two dimensions, control education.

1. Introduction

Magnetic levitation techniques have widely used in many engineering systems such as levitation of high speed trains, frictionless bearings, wind tunnels, and vibration isolation tables in semiconductor manufacturing. Magnetic levitation systems (MLSs) are nonlinear and open loop unstable. Therefore, they are excellent apparatus for testing different control schemes. MLSs are good educational tools in control engineering courses [1-17].

In recent years, the fuzzy sliding mode control (FSMC) is popular. The FSMC integrates the sliding mode control (SMC) and the fuzzy logic control (FLC) [18-20]. The SMC method can apply to a class of nonlinear systems in the global sense and consider robustness issues to modeling uncertainties and disturbances. The fuzzy set theory was introduced by Zadeh [20]. The FLC methods have been investigated for 40 years. They have been successfully adopted for many engineering applications. The FSMC provides a minimal fuzzy set of the FLC and a systematic design procedure [18-20]. It provides a simple way to achieve asymptotic stability of the system.

This paper proposes the two-dimensional fuzzy sliding mode control (2DFSMC) of the DSP-based magnetic levitation system. The sliding manifold and its derivative are both considered for fuzzy logic rules. For the experimental results, this method improves responses of the magnetic levitation system effectively.

This paper is outlined as follows. The SMC method is presented in Section 2. The FSMC strategy is stated in Section 3. The 2DFSMC is delineated in Section 4. The experiments and results are discussed in section 5. The conclusion is provided in Section 6.

2. Sliding Mode Control

The mathematical model of the DSP-based MLS is given as follows [1,2,4,7,15-17],

$$m\frac{d^2x}{dt^2} = mg - \frac{i^2}{h(x)} \tag{1}$$

where x is the distance between the electromagnet and the steel ball, m is the mass of the steel ball, g is the gravitational acceleration ,and i is the coil current. Let the magnetic

force be the function of $i^2/h(x)$. Let the measured output (v) of the ball position and the distance (x) have the following relationship

$$x = f(v) \tag{2}$$

The equation (1) becomes

$$m\frac{df}{dv}\frac{d^2v}{dt^2} = mg - \frac{i^2}{h(f(v))} \tag{3}$$

which implies

$$m'\frac{d^2v}{dt^2} = mg - \frac{i^2}{h'(v)} \tag{4}$$

where $m' = m\,df/dv$ and

$$h'(v) = h(f(v)) = a_4v^4 + a_3v^3 + a_2v^2 + a_1v + a_0 \tag{5}$$

Let v_1 be the position measurement, v_2 be its derivative and control input u be the coil current. Then the state equation of the DSP-based MLS is

$$\dot{v}_1 = v_2 \tag{6}$$

$$\dot{v}_2 = \frac{m}{m'}g - \frac{u^2}{m'h'(v_1)} \tag{7}$$

The control objective is to maintain the levitation height $v(t)$ at some desired height $v_0(t)$. Define the tracking error as

$$e(t) = v_1(t) - v_0(t) \tag{8}$$

For the tracking control, the sliding manifold can include an integral error term as follows

$$S(t) = \dot{e}(t) + c_1e(t) + c_2\int_0^t e(\tau)d\tau \tag{9}$$

The approaching and sliding condition of the $S(t) = 0$ manifold is

$$S(t)\dot{S}(t) < 0 \tag{10}$$

The derivative of $S(t)$ becomes

$$\dot{S}(t) = \ddot{e} + c_1\dot{e} + c_2 e$$

$$= (\dot{v}_2 - \ddot{v}_0) + c_1(v_2 - \dot{v}_0) + c_2(v_1 - v_0)$$

$$= \frac{m}{m'}g - \frac{u^2}{m'h'(v_1)} - \ddot{v}_0 + c_1(v_2 - \dot{v}_0) + c_2(v_1 - v_0) \tag{11}$$

The equivalent control law for $S(t) = 0$ can be obtained as follows [2]

$$u_{eq}^2 = m'h'(v_1)\{\frac{m}{m'}g - \ddot{v}_0 + c_1(v_2 - \dot{v}_0) + c_2(v_1 - v_0)\} \tag{12}$$

and the overall sliding mode control u_{sm} is determined by

$$u_{sm}^2 = m'h'(v_1)\{\frac{m}{m'}g - \ddot{v}_0 + c_1(v_2 - \dot{v}_0) + c_2(v_1 - v_0) + \eta \cdot sign(S(t))\} \tag{13}$$

where η is a positive real number and the sign function $sign(\bullet)$ is

$$sign(S(t)) = \begin{cases} 1, & \text{if } S(t) > 0 \\ -1, & \text{if } S(t) < 0 \\ 0, & \text{if } S(t) = 0 \end{cases} \tag{14}$$

Substituting (13) into $S(t)\dot{S}(t)$, we can obtain [2]

$$S(t)\dot{S}(t) = -\eta|S(t)| < 0 \tag{15}$$

So the controller (13) satisfies the approaching and sliding condition (10). For steady states, the error $e(t)$ and the error integral $\int_0^t e(\tau)d\tau$ approach to zero. There may be chatters due to $sign(\bullet)$ function. This chattering problem can be improved by using control smoothing approximations. One possible method is to replace the function $sign(\bullet)$ with the function $sat(\bullet)$ as follows

$$sat\left(S(t)/\phi\right) = \begin{cases} sign(S(t)), & \text{if } |S(t)| \geq \phi \\ S(t)/\phi, & \text{if } |S(t)| < \phi \end{cases} \tag{16}$$

where ϕ is the band parameter and is a positive real number.

3. Fuzzy Sliding Mode Control

The linguistic sets of the universe of discourse S/ϕ_f and the fuzzy control output u_{fz} have the form: positive big (PB), positive middle (PM), positive small (PS), zero (ZE), negative small (NS), negative middle (NM) and negative big (NB). The membership functions of these fuzzy sets are shown in Fig. 1.

From (13), the FSMC is determined by

$$u_{fsm}^2 = m'h'(v_1)\{\frac{m}{m'}g - \ddot{v}_0 + c_1(v_2 - \dot{v}_0) + c_2(v_1 - v_0) + \eta_f \cdot u_{fz}\left(S/\phi_f\right)\} \qquad (17)$$

where η_f is the denormalized factor of FSMC and ϕ_f is the normalized factor of S. The fuzzy inference rules are conveniently described as follows,

Rule 1: IF S/ϕ_f is PB, THEN u_{fz} is PB,

Rule 2: IF S/ϕ_f is PM, THEN u_{fz} is PM,

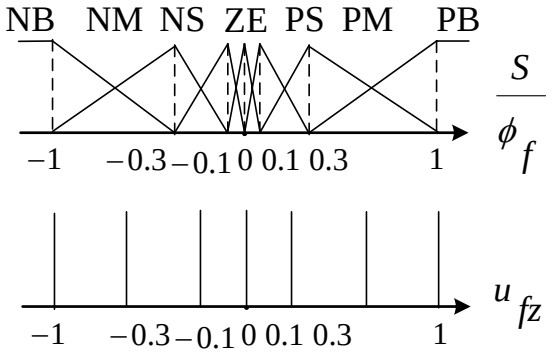

Fig. 1 The membership functions of the sliding manifold and the fuzzy control

Rule 3: IF S/ϕ_f is PS, THEN u_{fz} is PS,

Rule 4: IF S/ϕ_f is ZE, THEN u_{fz} is ZE,

Rule 5: IF S/ϕ_f is NS, THEN u_{fz} is NS,

Rule 6: IF S/ϕ_f is NM, THEN u_{fz} is NM,

Rule 7: IF S/ϕ_f is NB, THEN u_{fz} is NB.

The centroid defuzzification method calculates the weighted average of fuzzy set. The result of applying centroid defuzzification to a fuzzy conclusion can be expressed by the formula

$$u_{fz} = \frac{\sum_{n=1}^{7} \mu_n\left(S/\phi_f\right) \times u_{fz}(n)}{\sum_{n=1}^{7} \mu_n\left(S/\phi_f\right)} \tag{18}$$

where n is the rule number and $\mu_n(\bullet)$ is the membership function.

Substituting (17) into $S(t)\dot{S}(t)$, we can obtain

$$\begin{aligned} & S(t)\dot{S}(t) \\ &= S(t)\cdot\left\{\frac{m}{m'}g - \frac{u_{fsm}^2}{m'h'(v_1)} - \ddot{v}_0 + c_1\left(v_2 - \dot{v}_0\right) + c_2\left(v_1 - v_0\right)\right\} \\ &= -\eta_f S \cdot u_{fz}\left(S/\phi_f\right) \le 0 \end{aligned} \tag{19}$$

From *Rule 1* to *Rule 7*, the sliding manifold S and fuzzy control u_{fz} are in phase. So the controller (17) satisfies the approaching and sliding condition (10).

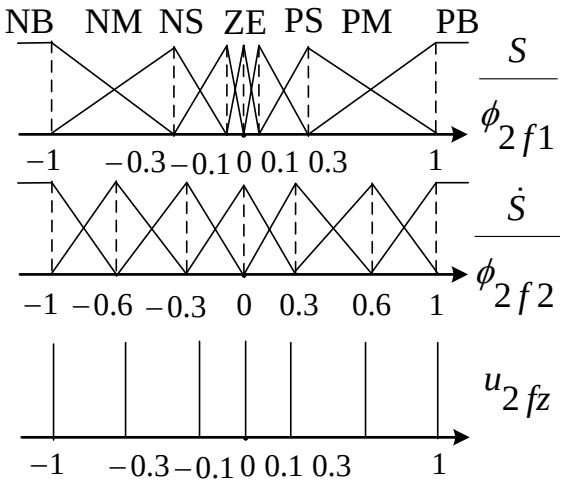

Fig. 2 The membership functions of the 2DFSMC

4. Two-Dimensional Fuzzy Sliding Mode Control

In this section, the two-dimensional fuzzy sliding mode control (2DFSMC) is proposed. The 2DFSMC method is to check both of the sliding manifold S and its derivative $\dot{S}$ simultaneously. From (13) and (17), the 2DFSMC is determined by

$$u_{2fsm}^{2} = m'h'(v_1)\{\frac{m}{m'}g - \ddot{v}_0 + c_1(v_2 - \dot{v}_0) + c_2(v_1 - v_0) + \eta_{2f} \cdot u_{2fz}\left(\frac{S}{\phi_{2f1}}, \frac{\dot{S}}{\phi_{2f2}}\right)\} \quad (20)$$

where $u_{2fz}\left(S/\phi_{2f1}, \dot{S}/\phi_{2f2}\right)$ is the fuzzy function of S/ϕ_{2f1} and $\dot{S}/\phi_{2f2}$. η_{2f} is the denormalized factor, ϕ_{2f1} is the normalized factor of S ,and ϕ_{2f2} is the normalized factor of $\dot{S}$. Comparing (13), (17) and (20), the difference is the last term. The main function of the last term is switching. The design criterion is to make the derivative of Lyapunov function negative. The fuzzy numbers S/ϕ_{2f1}, $\dot{S}/\phi_{2f2}$ and u_{2fz} are chosen from the set of fuzzy numbers that represent the linguistic states PB, PM, PS, ZE, NS, NM and NB. They are depicted in Fig. 2. The total number of possible non-conflicting fuzzy inference rules is 49. They can conveniently be represented in Table 1. In the previous section, only one proposition S/ϕ_f is concerned. It is so called one-dimensional fuzzy sliding mode control. Taking Table 1 into account, both of S/ϕ_{2f1} and $\dot{S}/\phi_{2f2}$ are concerned. Hence, it is called two-dimensional fuzzy sliding mode control.

For the defuzzifier, the same centroid defuzzification method is used as follows,

Table 1 Rules of the 2DFSMC

u_{2fz}	S/ϕ_{2f1}							
$\dot{S}/\phi_{2f2}$		**NB**	**NM**	**NS**	**ZE**	**PS**	**PM**	**PB**
	PB	***ZE***	***PS***	***PM***	***PM***	***PB***	***PB***	***PB***
	PM	***NS***	***ZE***	***PS***	***PS***	***PM***	***PM***	***PB***
	PS	***NM***	***NS***	***ZE***	***PS***	***PS***	***PM***	***PB***
	ZE	***NM***	***NS***	***NS***	***ZE***	***PS***	***PS***	***PM***
	NS	***NB***	***NM***	***NS***	***NS***	***ZE***	***PS***	***PM***
	NM	***NB***	***NM***	***NM***	***NS***	***NS***	***ZE***	***PS***
	NB	***NB***	***NB***	***NB***	***NM***	***NM***	***NS***	***ZE***

$$u_{2fz}=\frac{\sum_{n=1}^{49}\mu_n\left(\frac{S}{\phi_{2f1}}\times\frac{\dot{S}}{\phi_{2f2}}\right)\times u_{2fz}(n)}{\sum_{n=1}^{49}\mu_n\left(\frac{S}{\phi_{2f1}}\times\frac{\dot{S}}{\phi_{2f2}}\right)} \tag{21}$$

where the inferred membership function is $\mu_n\left(\frac{S}{\phi_{2f1}}\times\frac{\dot{S}}{\phi_{2f2}}\right)=\min\left[\mu_n\left(\frac{S}{\phi_{2f1}}\right),\ \mu_n\left(\frac{\dot{S}}{\phi_{2f2}}\right)\right]$.

Substituting (20) into $S(t)\dot{S}(t)$, we can obtain

$$\begin{aligned}&S(t)\dot{S}(t)\\&=S(t)\cdot\left\{\frac{m}{m'}g-\frac{u_{2fsm}^2}{m'h'(v_1)}-\ddot{v}_0+c_1(v_2-\dot{v}_0)+c_2(v_1-v_0)\right\}\\&=-\eta_{2f}S\cdot u_{2fz}\left(\frac{S}{\phi_{2f1}},\frac{\dot{S}}{\phi_{2f2}}\right)\end{aligned} \tag{22}$$

Referring to Table 1, the diagonal linguistic states are all ZE. The upper triangular linguistic states are all positive and the lower triangular linguistic states are all negative. If Table1 is viewed as a plane, the horizontal axis is S and the vertical axis is approximated to the derivative of S, then the diagonal line is

$$\frac{S}{\phi_{2f1}}+\frac{\dot{S}}{\phi_{2f2}}=0 \tag{23}$$

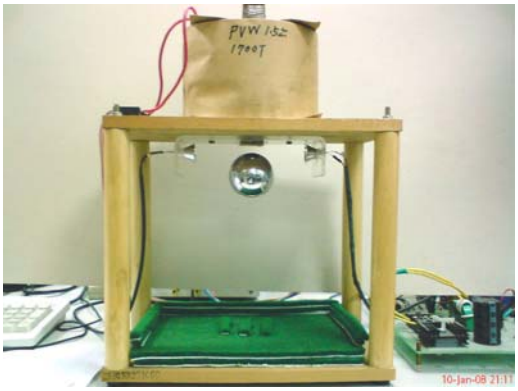

Fig. 3 The experimental setup of the DSP-based MLS

Hence, the fuzzy conclusion of u_{2fz} is

$$\begin{cases} u_{2fz} > 0, \text{ if } \dfrac{S}{\phi_{2f1}} + \dfrac{\dot{S}}{\phi_{2f2}} > 0 \\ u_{2fz} = 0, \text{ if } \dfrac{S}{\phi_{2f1}} + \dfrac{\dot{S}}{\phi_{2f2}} = 0 \\ u_{2fz} < 0, \text{ if } \dfrac{S}{\phi_{2f1}} + \dfrac{\dot{S}}{\phi_{2f2}} < 0 \end{cases} \tag{24}$$

and is similar with the $sat(\bullet)$ function (16). By rearranging (23), we can obtain

$$\dot{S}(t) = -\frac{\phi_{2f2}}{\phi_{2f1}} S(t) \tag{25}$$

Substituting (22) for (25), we can obtain

$$S(t) \cdot \dot{S}(t) = -\frac{\eta_{2f}\phi_{2f2}}{\phi_{2f1}} S^2(t) \le 0 \tag{26}$$

So the controller (20) satisfies the approaching and sliding condition (10).

5. Experiments and Results

The experimental setup of DSP-based MLS is shown in Fig. 3. Its implemented circuits are shown in Fig. 4. The left circuit of Fig. 4 is the coil current sensor and driver. The IGBT (Insulated Gate Bipolar Transistor) is served as a switch of PWM. The TLP 250 is an IGBT trigger IC (Integrated Circuit). The PWM control is from eZdsp F2812 [21] PWM port. When the IGBT is off, open-circuit can be avoided by the flywheel diode. The current transducer LA55-P is a Hall element and transfers current signal to voltage signal. The coil current signal is sampled by the eZdsp F2812 A/D port. The sample rate is 1K Hz. The right circuit of Fig. 4 is the position sensor of steel ball. The blue diode is an emitter and the white diode is a receiver. When the steel ball is at the middle of the diodes, the output voltage is 1.5 Volts. It is the position where the steel ball is 0.7 cm away from the electromagnet as shown in Fig. 5.

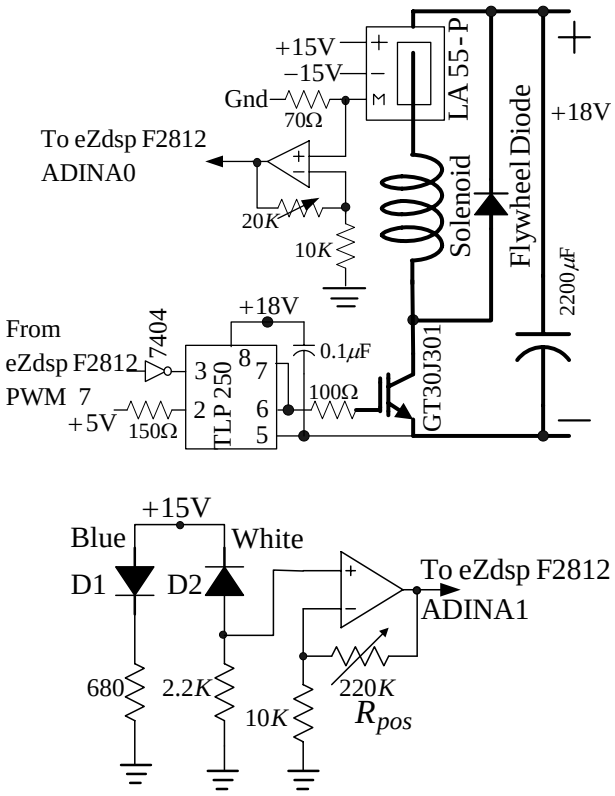

Fig. 4 The implemented circuits of the DSP-based MLS

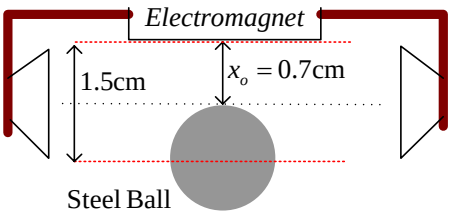

Fig. 5 The steel ball and sensor diagram

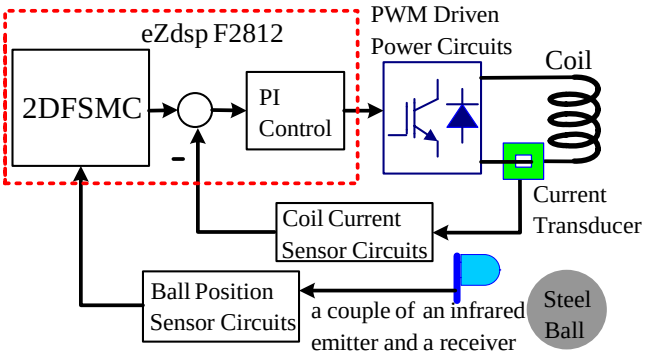

Fig. 6 The function diagram of the DSP-based MLS

The total function diagram of the DSP-based MLS is shown in Fig. 6. There are two control loops in this diagram. The inner loop is used to compensate the coil current and the outer loop is served as the ball position control. This control technique is very popular for control of mechatronics. It is named multiloop control [4]. The coil current is well

compensated by PI (Proportional and Integral) controller [16,17]. Fig. 7 is the step response of the coil current from 1 Amp to 2 Amps. From Fig. 7, the settling time of the coil current is about 50ms. The dynamics of coil current is faster than that of position, so the gain can be approximated as 1. When the inner loop design is accomplished, the outer loop design can be started.

The first experiment is to measure the characteristic curve of the MLS. From [16], the PD (Proportional and Derivative) control can be used to stabilize the MLS.

Table 2 Measured data

Set point	Current	position
No.1	0.93 A	0.5 V
No.2	1.15 A	1　V
No.3	1.26 A	1.5 V
No.4	1.36 A	2　V
No.5	1.52 A	2.5 V

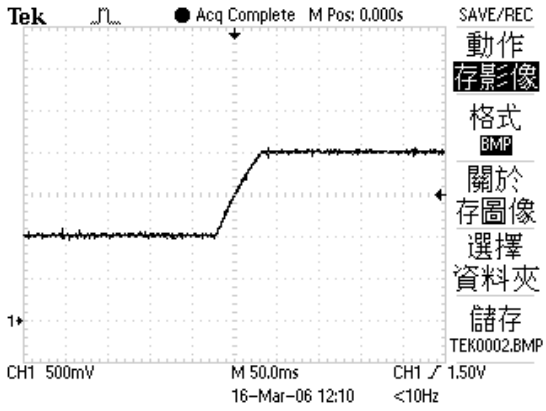

Fig. 7 The coil current response

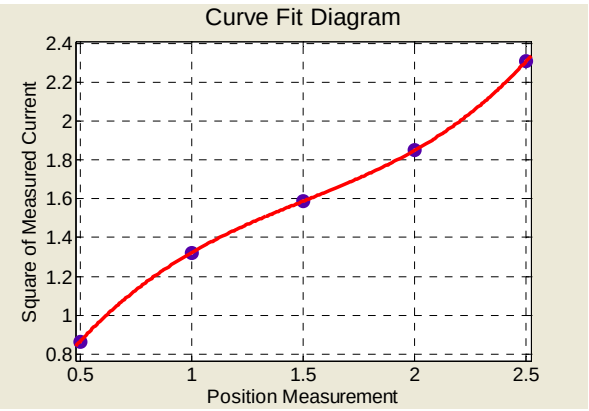

Fig. 8 The fitting curve of the easuredposition and he current

The corresponding stable input-output data are shown in Table 2. The characteristic curve is

shown in Fig. 8. The x-axis is the position measurement and the y-axis is the square of coil current. The fitting curve of Fig. 8 is

$$\begin{aligned} i^2 &= mgh'(v) \\ &= \bar{a}_4 v^4 + \bar{a}_3 v^3 + \bar{a}_2 v^2 + \bar{a}_1 v + \bar{a}_0 \end{aligned} \tag{27}$$

where $\bar{a}_4 = 0.008333,\ \bar{a}_3 = 0.2109,\ \bar{a}_2 = -1.07,\ \bar{a}_1 = 2.135,\ \bar{a}_0 = 0.0379.$

Because the velocity of the magnet is not available, the approximation $v_2 \approx \dfrac{\Delta v_1(k)}{\Delta t} = \dfrac{v_1(k) - v_1(k-1)}{1ms}$ is made. Hence the equations (9), (13), and (16) are modified as follows,

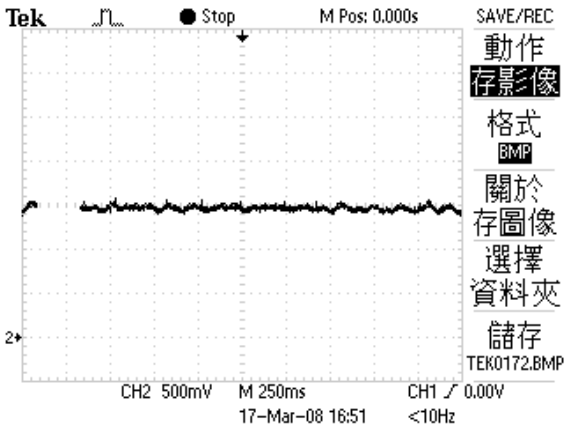

Fig. 9 The set point response of 2DFSMC

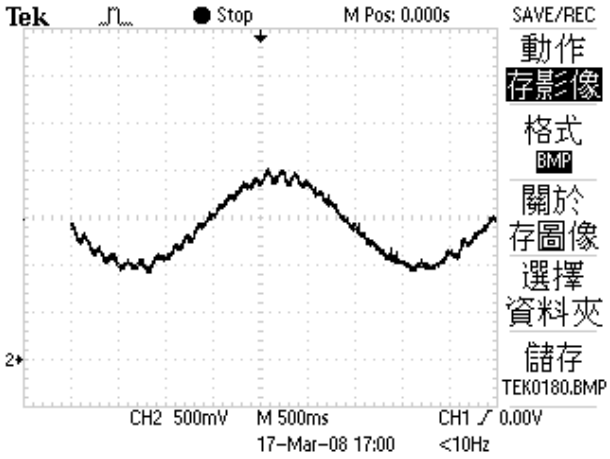

Fig. 10 The sinusoidal response of 2DFSMC

$$\tilde{S}(k) = \frac{\Delta e(k)}{1ms} + c_1 e(k) + c_2 \sum_{n=0}^{k} e(n) \cdot 1ms \tag{28}$$

$$\begin{aligned} u_{sm}^2(k) &= mgh'(v_1)\{1 + \frac{c_1}{g}\frac{m'}{m}\frac{\Delta v_1(k)}{1ms} + \frac{c_2}{g}\frac{m'}{m}e(k) + \frac{\eta}{g}\frac{m'}{m}sat(\tilde{S}(k)/\phi)\} \\ &= mgh'(v_1)\{1 + c_1'\Delta v_1(k) + c_2' e(k) + \eta' sat(\tilde{S}(k)/\phi)\} \end{aligned} \tag{29}$$

where $c_1' = \dfrac{c_1}{g}\dfrac{m'}{m}\dfrac{1}{1ms},\ c_2' = \dfrac{c_2}{g}\dfrac{m'}{m},\ \eta' = \dfrac{\eta}{g}\dfrac{m'}{m}.$

The FSMC based on (28) , (29) and (17) is modified as follows

$$u_{fsm}^{2}(k) = mgh'(v_1)\{1 + c_1'\Delta v_1(k) + c_2' e(k) + \eta_f' \cdot u_{fz}\left(\frac{\tilde{S}(k)}{\phi_f}\right)\} \qquad (30)$$

where $\eta_f' = \frac{\eta_f}{g}\frac{m'}{m}$.

The 2DFSMC (20) is modified as follows

$$u_{2fsm}^{2}(k) = mgh'(v_1)\{1 + c_1'\Delta v_1(k) + c_2' e(k) + \eta_{2f}' \cdot u_{2fz}\left(\frac{\tilde{S}(k)}{\phi_{2f1}}, \quad \frac{\Delta\tilde{S}(k)}{\phi_{2f2}}\right)\} \qquad (31)$$

where $\eta_{2f}' = \frac{\eta_{2f}}{g}\frac{m'}{m}$ and $\Delta\tilde{S}(k) = \tilde{S}(k) - \tilde{S}(k-1)$.

The experimental results are shown in figures 9, 10 and 11. The control parameters are given as follows: $c_1' = 3.00$, $c_2' = 0.48$, $\phi_{2f1} = 1.2$, $\phi_{2f2} = 1.0$, $\eta_{2f}' = 0.01$. Fig. 9 is the ball position response of 2DFSMC. The set point is 1.5 Volts. There is no steady state error in this set point experiment because of the integral error control term.

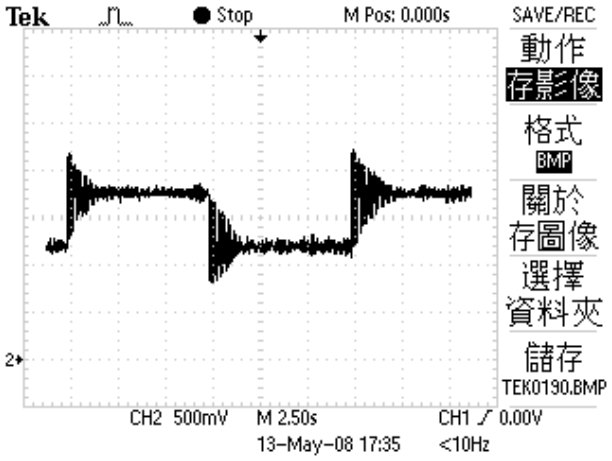

Fig. 11 The step response of 2DFSMC

Fig. 10 shows the sinusoidal response of 2DFSMC. The input signal is $1.5 + 0.5\sin\frac{2\pi t}{3}$.

This result guarantees that 2DFSMC can deal with system nonlinearity. From Fig. 10, the sinusoidal distortion is almost null. In fact, 3 Hz operation frequency is the highest frequency for normal operation. The controller can not track the sinusoidal command which is faster than 4 Hz. The step response is shown in Fig. 11. It is shown in the form of square wave. The

average is 1.5Volts. The amplitude is 1 Volt. From Fig. 11, the system response is under-damped. This is a common phenomenon for magnetic levitation systems. In this case, the controller is employed to improve the system damping. However, 2DFSMC stabilizes the magnetic levitation system successfully.

6. Conclusions

The main contribution of this paper is the 2DFSMC of DSP-based MLS. The sliding manifold and its derivative are both considered for fuzzy rules. For the experimental results, this method improves responses of the magnetic levitation system effectively. These experiments are appropriate for control education.

References

[1] H. Wong, "Design of a magnetic levitation control system — an undergraduate project," IEEE Transactions on Education, Vol.29, No.4, pp.196-200, 1986.

[2] D. Cho, Y. Kato and D. Spilman, "Sliding mode and classical controllers in magnetic levitation systems", IEEE Control System Magazine, Vol.13, No.1, pp.42-48, 1993.

[3] M. Fujita, T. Namerikawa, F. Matsumura, and K. Uchida, "μ-Synthesis of an electromagnetic suspension system," IEEE Transactions on Automatic Control, Vol.40, No.3, pp.530-536, 1995.

[4] J.-H. Li and T.-H. S. Li, "Multiloop control of thyristor-driven magnetic levitation system," Mechatronics, Vol. 5, No.5, pp.469-481, 1995.

[5] S. Mittal, and C.-H. Menq, "Precision motion control of a magnetic suspension actuator using a robust nonlinear compensation scheme," IEEE/ASME Transactions on Mechatronics, Vol.2, No.4, pp.268-280, 1997.

[6] W. G. Hurley and W. H. Wolfle, "Electromagnetic design of a magnetic suspension system," IEEE Transactions on Education, Vol. 40, No. 2, pp.124-130, 1997.

[7] J.-L. Lin and B.-C. Tho, "Analysis and μ– based controller design for an electromagnetic suspension system," IEEE Transactions on Education, Vol. 41, No. 2, pp.116-129, 1998.

[8] V. A. Oliveira, E. F. Costa, and J. B. Vargas, "Digital implementation of a magnetic suspension control system for laboratory experiments," IEEE Transactions on Education,

Vol. 42, No. 4, pp. 315-322, 1999.

[9] A. E. Hajjaji and M. Ouladsine, “Modeling and nonlinear control of magnetic levitation systems,” IEEE Transactions on Industrial Electronics, Vol.48, No.4, pp.831-838, 2001.

[10] P. S. Shiakolas and D. Piyabongkarn, “Development of a real-time digital control system with a hardware-in-the-loop magnetic levitation device for reinforcement of controls education,” IEEE Transactions on Education, Vol. 46, No. 1, pp.79-87, 2003.

[11] G. Marsden, “Levitation,” Nuts and Volts Magazine, Vol.24, No.9, pp.58-61, 2003.

[12] K. H. Lundberg, K. A. Lilienkamp, and G. Marsden, “Low-cost magnetic levitation project kits,” IEEE Control System Magazine, Vol.24, No.5, pp.65-69, 2004.

[13] P. S. Shiakolas, S. R. VanSchenck, D. Piyabongkarn, and I. Frangeskou, “Magnetic levitation hardware-in-the-loop and matlab-based experiments for reinforcement of neural network control concepts,” IEEE Transactions on Education, Vol. 47, pp.33-41, 2004.

[14] W. G. Hurley, M. Hynes ,and W. H. Wolfle, “PWM control of a magnetic suspension system,” IEEE Transactions on Education, Vol. 47, No. 2, pp. 165-173, 2004.

[15] V. A. Oliverira, E. S. Tognetti, and D. Siqueira, “Robust controllers enhanced with design and implementation processes,” IEEE Transactions on Education, Vol.49, No.3, pp.370-382, 2006.

[16] J.-H. Li, “An undergraduate digital control project: a digital signal processor (DSP)-based magnetic levitation system,” World Transactions on Engineering and Technology Education, Vol. 5, No.1, pp.207-210, 2006.

[17] J.-H. Li, “Fuzzy supervisory control of a dsp-based magnetic levitation system”, Asian Journal of Control, Vol.9, No.1, pp.64-67, 2007.

[18] R. Palm, “Robust control by fuzzy sliding mode”, Automatica, Vol.30, No.9, pp.1429-1437, 1994.

[19] S. W. Kim and J. J. Lee, “Design of a fuzzy controller with fuzzy sliding surface”, Fuzzy Sets and Systems, Vol.71, No.3, pp.359-367, 1995.

[20] L.-X. Wang, A course in fuzzy systems and control, Prentice-Hall, New Jersey, 1997.

[21] Texas Instruments Inc. Available: www.ti.com